

## Supporting Information for

On the discovery of hyper-hydrated sodium chloride hydrates, stable at icy moon conditions.

Baptiste Journaux<sup>1\*</sup>, Anna Pakhomova<sup>2,3</sup>, Ines E. Collings<sup>3,4</sup>, Sylvain Petitgirard<sup>5</sup>, Tiziana Boffa Balaran<sup>6</sup>, J. Michael Brown<sup>1</sup>, Steve D. Vance<sup>7</sup>, Stella Chariton<sup>8</sup>, Vitali .B. Prakapenka<sup>8</sup>, Dongyang Huang<sup>5</sup>, Jason Ott<sup>1</sup>, Konstantin. Glazyrin<sup>2</sup>, Gaston Garbarino<sup>3</sup>, Davide. Comboni<sup>3</sup>, Michael. Hanfland<sup>3</sup>.

<sup>1</sup>Department of Earth and Space Sciences, University of Washington; Seattle, WA 98195, USA.

<sup>2</sup>Deutsches Elektronen-Synchrotron, D-22607 Hamburg, Germany

<sup>3</sup>European Synchrotron Radiation Facility; 38000 Grenoble, France.

<sup>4</sup>Center for X-ray Analytics, Empa - Swiss Federal Laboratories for Materials Science and Technology, Überlandstrasse 129, 8600 Dübendorf, Switzerland.

<sup>5</sup>Institute of Geochemistry and Petrology, ETH Zürich, 8092 Zürich, Switzerland.

<sup>6</sup>Bayerisches Geoinstitut, University of Bayreuth, 95440 Bayreuth, Germany.

<sup>7</sup>Jet Propulsion Laboratory, California Institute of Technology, Pasadena, CA 91109, USA.

<sup>8</sup>Center for Advanced Radiation Sources, University of Chicago, Chicago, IL, USA.

\*Corresponding author

**Email:** [bjournau@uw.edu](mailto:bjournau@uw.edu)

### This PDF file includes:

Supporting text  
Figures S1 to S7  
Tables S1 to S4  
Legends for Datasets S1  
SI References

### Other supporting materials for this manuscript include the following:

Datasets S1

## Supporting Information Text

### S1. Pressure – Temperature experimental path

In Experiment 1, we started by cooling down the NaCl(aq) solution at 500 MPa down to 240 K. After formation of needles of the C2/c hydrate, the pressure was decreased down to 400 MPa and the C2/c phase transformed to SC8.5.

In Experiment 2, we started by cooling down the NaCl(aq) solution at 300 MPa down to 220 K where SC8.5 crystallized. We then increased pressure and temperature gradually up to 600 MPa and 255 K to follow the liquidus of SC8.5. Afterwards, at the same pressure, the temperature was raised up to 300 K and the SC8 crystals melted. The aqueous solution was then brought to 1500 MPa where it was cooled down to 270 K, causing SC13 to crystallize. We then explored the melting curve of SC13 up to 2 GPa and 300 K.

In Experiment 3, we started by cooling the NaCl(aq) solution at 360 MPa down to 240 K where SC8.5 was formed coexisting with ice II. Pressure and temperature were then gradually risen to 1230 MPa and 274 K, conditions at which SC8.5 was still present. At 274 K and 1230 MPa, upon warming, the SC8.5 crystals transformed into an ice VI + SC2 assemblage. This suggests that SC8.5 is not stable above 274 K. After rising the pressure to 1550 MPa and the temperature to 290 K, SC13 formed from the ice VI + SC2 assemblage and remained stable up to 2140 MPa and 300 K. We completely melted SC13 at 1600 MPa and 300 K while retaining a crystal of ice VI, demonstrating that ice VI is the stable phase at the liquidus at 4 mol/kg NaCl concentration. Upon cooling of the ice VI + brine, the brine froze into SC2 at 250 K. As we previously observed SC13 at higher temperature (up to 274 K), we expect that the hydrohalite crystallised at 250 K is metastable and formed because we reached the metastable ice VI – SC2 – aqueous solution eutectic by supercooling the solution and increasing its NaCl content while following the ice VI liquidus. Finally, the SC2 + ice VI assemblage was further compressed above 2000 MPa where it transformed into ice VII + NaCl.

In Experiment 4, we formed the C2/c needle hydrate upon cooling down the NaCl(aq) solution to 240 K at 300 MPa. The C2/c phase eventually transformed into SC8.5 at the same conditions after 20 minutes. Temperature and pressure were cycled to obtain a single crystal of SC8.5. This single crystal was then cooled down to 150 K and the pressure in the DAC membrane was brought back to 0. The residual pressure in the cell was measured to be 30 MPa and the presence of SC8.5 + ice Ih was detected using powder X-Ray diffraction. The temperature was then gradually raised until we observed a transition to ice Ih + SC2 (hydrohalite) between 210 and 240 K.

Coordinate of experimental points are given in Table S1.

### S2. Structure Solution and refinements

The crystal structures of the two NaCl hydrates, 2NaCl·17H<sub>2</sub>O (SC8.5) and NaCl·13H<sub>2</sub>O (SC13), were solved using a dual-space algorithm implemented in the SHELXT program (1). The iterative structure refinements were performed with the use of the SHELXL program (1) built in the ShelXle (2) graphical user interfaces. Thermal displacement parameters for Na, Cl and O atoms were refined in anisotropic approximation. Only H positions that could be identified in the Fourier difference maps were included in the refinement. The O-H bond distances were constrained to be 0.85 Å. The displacement parameters of hydrogens were constrained to be 1.2 times the isotropic parameters of the corresponding oxygens. Bragg reflections overlapping with reflections from the diamonds were excluded from the structure analysis. The details of structure refinements are given in Table S2 as well as in Text S2.1 and Text S2.2. The Crystallographic Information Files (CIFs) for the reported structures are deposited as Supporting Information as well as in the Inorganic Crystal Structure Database (ICSD) under deposition numbers CSD 2203504-2203505.

**Structure refinement of 2NaCl·17H<sub>2</sub>O (SC8.5).** The presented structural data were collected on a selected crystal at P = 450 MPa and T = 243 K (Figure 1b) in the Experiment 2. The monoclinic crystal of SC8.5 (2NaCl·17H<sub>2</sub>O), with unit-cell lattice parameters  $a = 15.0132(4)$  Å,  $b = 6.08030(10)$  Å,  $c = 21.9946(18)$  Å and  $\beta = 103.086(5)^\circ$  and space group C2/c, formed with two twin

domains having almost equal proportion and related by 180° along the [010] direction. Since there was minimal overlap between the two domains, the structure was solved by integrating only one of the domains. The reciprocal space reconstructions are given in **Erreur ! Source du renvoi introuvable.** The refined hydrogen bonding scheme is reported in Table S3 and Figure S2.

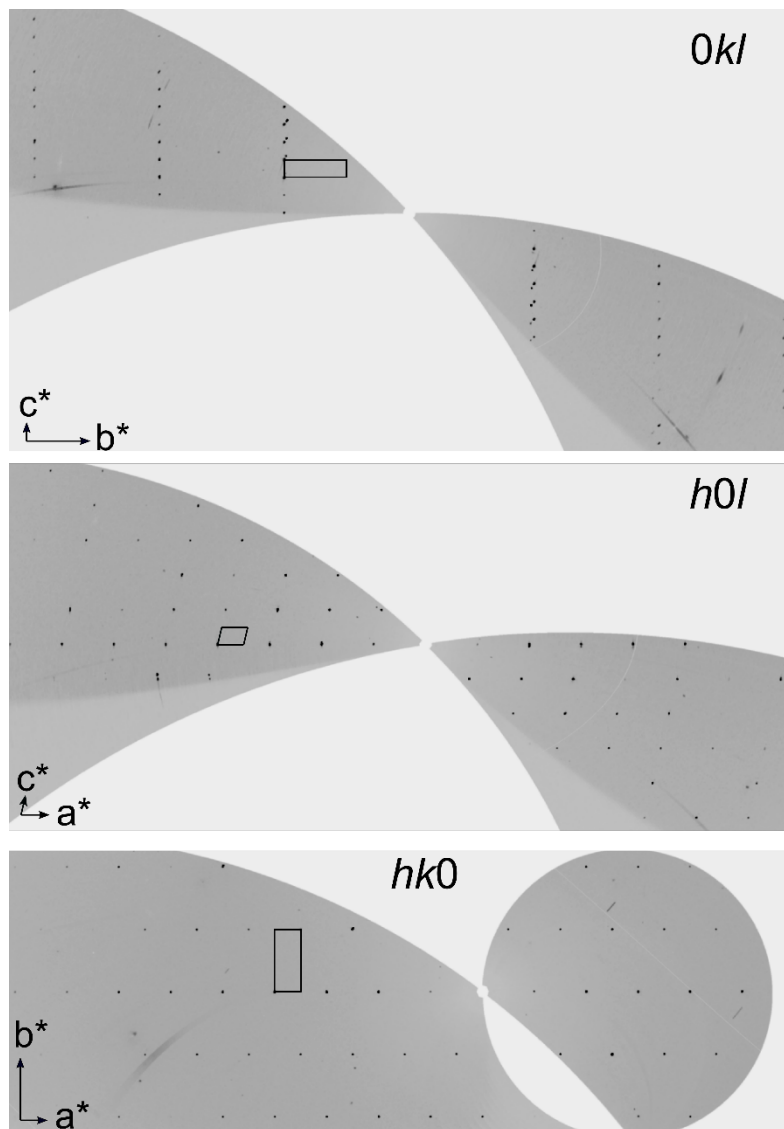
**Structure refinement of NaCl·13H<sub>2</sub>O (SC13).** The presented structural data were collected on a selected crystal at P = 1500 MPa and T = 295 K (Figure 1d) in the Experiment 2. The monoclinic crystal of SC13 (NaCl·13H<sub>2</sub>O), with the unit-cell lattice parameters  $a = 10.9150(8)$  Å,  $b = 11.8900(10)$  Å,  $c = 11.2752(5)$  Å and  $\beta = 118.307(7)^\circ$  and space group  $I2/m$ , formed with two twin domains but with one domain being prominent (~75%). Since there was minimal overlap between the two domains, the structure was solved by integrating the dominant domain. The reciprocal space reconstructions are given in Fig.S3. The refined hydrogen bonding scheme is reported in Table S4 and Figure S4.

### S3. Thermodynamic analysis

**Hydrate SC8.5 metastable liquidus at 1 bar.** Liquidus points from our data at 4 mol/kg NaCl concentration and from Valenti et al., (2012) at 5.7 mol/kg NaCl concentration were used to constrain the SC8.5 PTX liquidus surface. We used Sawamura et al., (2007) data to constrain the PTX liquidus curve of hydrohalite. The data were fitted using the thermodynamic surfaces fitting framework (Local basis function) from Brown, (2018) in order to provide reasonable extrapolated behavior with the trend observed in the data. The SC8.5-SC2-metastable liquid triple point is the intersection of the two surfaces at 1 bar. We estimate its coordinates at 235 K and 4.5 mol/kg.

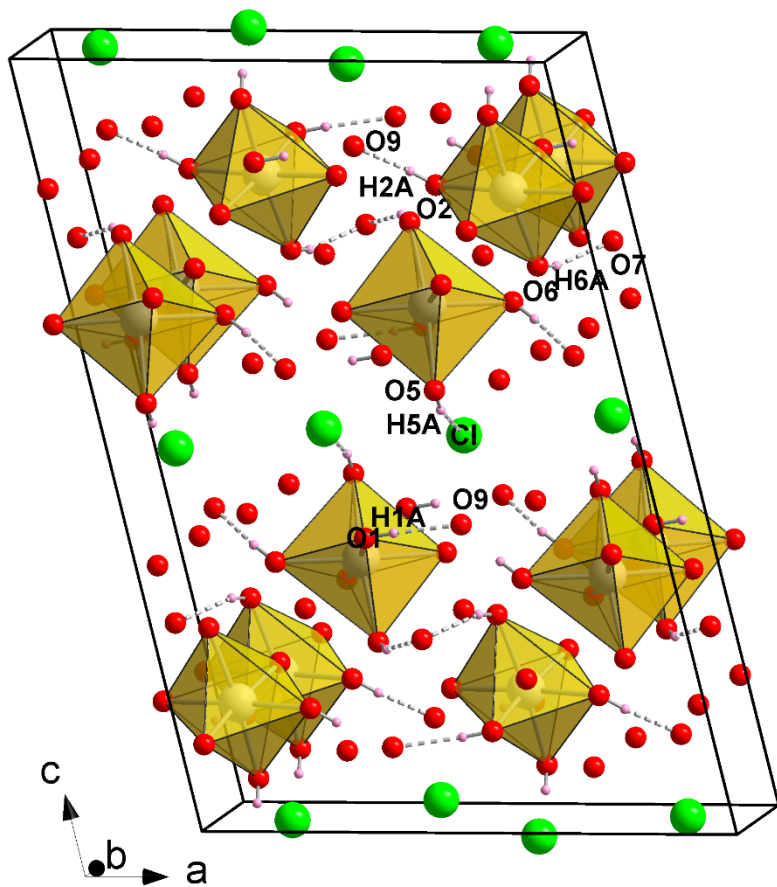
**H<sub>2</sub>O-NaCl phase diagram at high pressure.** Figure S7 illustrate possible phase diagrams for H<sub>2</sub>O-NaCl at 400 and 1500 MPa compatible with the information collected in the present study. Melting points of ice polymorphs at 400 MPa and 1500 MPa, as well as the stoichiometric composition of hydrate phases are definite constrains. Exact positions of equilibrium transition curves like liquidus (dashed), eutectic points (E, green triangle) and peritectic points (P<sub>n</sub>, black circles) remain uncertain with available thermodynamic data. At 1500 MPa, the stability field of SC13 must be small as it must be above 4 mol/kg (ice VI was stable at the liquidus) and below 4.3 mol/kg, the stoichiometric composition of SC13. Lower solubility concentrations of NaCl and SC2 with increasing pressure above 400 MPa have been reported by Adams, (1931) up to 1700 MPa. Exploration of phase stability, notably liquidus coordinates of ices and hydrates at high pressure is required to further refine the boundaries of the H<sub>2</sub>O-NaCl phase diagram.

Fig. S1.



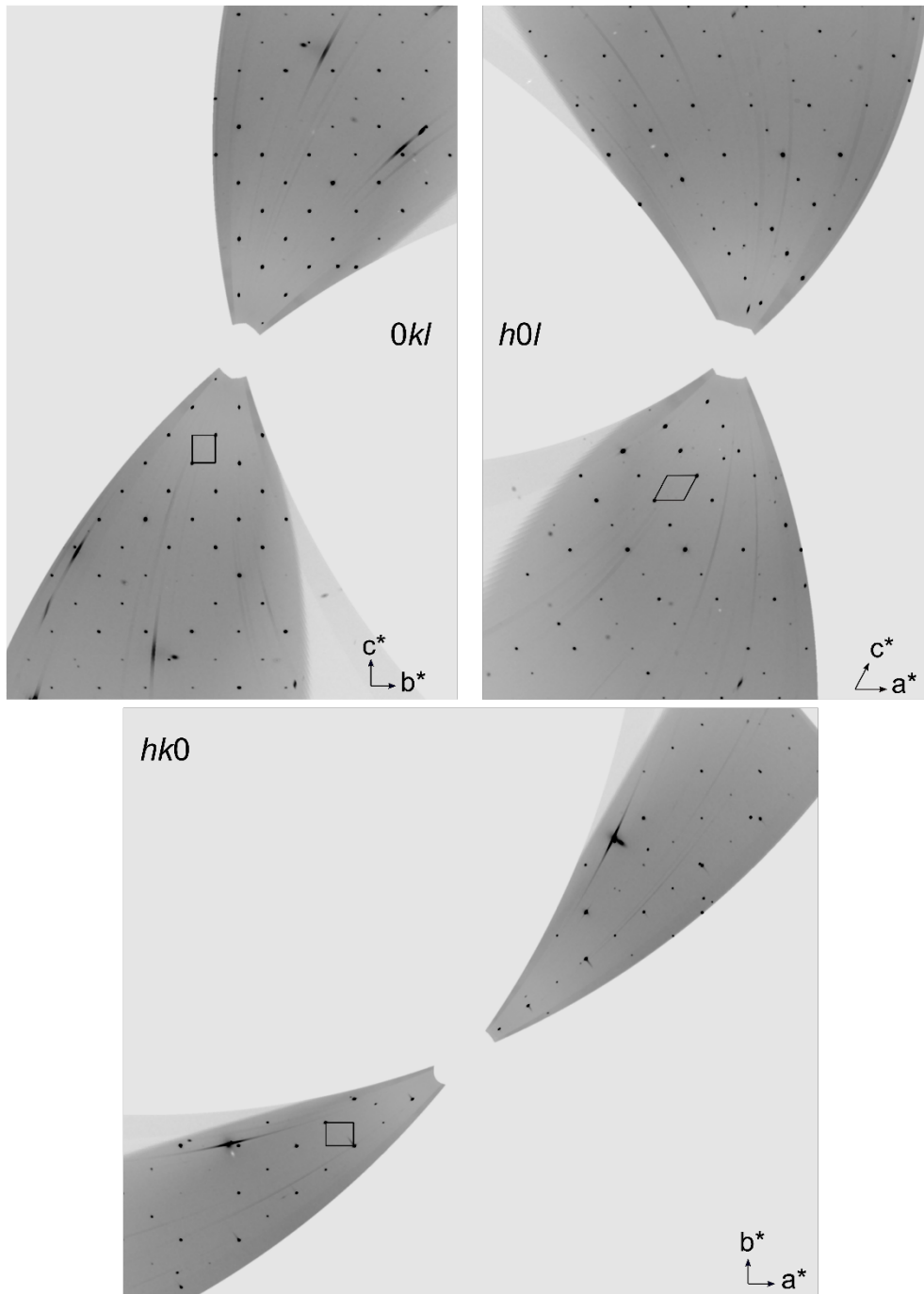
Reciprocal space reconstructions with the reciprocal unit cell indicated of 2NaCl·17H<sub>2</sub>O at 0.45 GPa and 243 K, measured at ID15B beamline at the ESRF. In the 0kl reconstruction, the presence of the second twin domain can be observed.

Fig. S2.



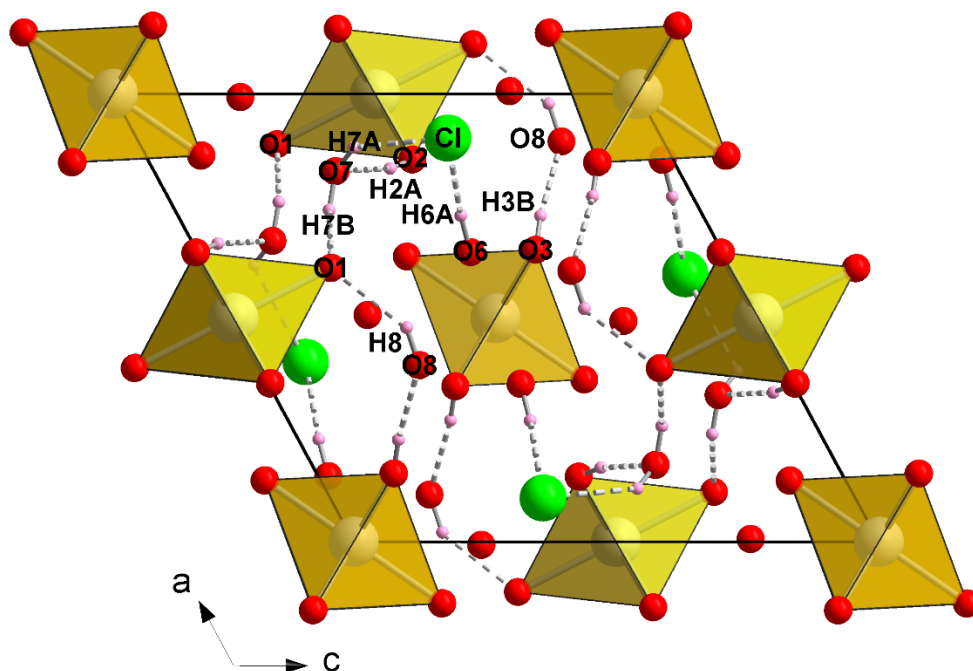
Crystal structure of disodium chloride decaheptahydrate 2NaCl·17H<sub>2</sub>O (SC8.5). [Na(H<sub>2</sub>O)<sub>6</sub>]<sup>+</sup> units are represented by yellow colored octahedra; the spheres represent locations of Na<sup>+</sup> (yellow), Cl<sup>-</sup> (green) and, O (red), and solved hydrogen positions in pink. The dashed grey lines represent hydrogen bonding.

Fig.S3.



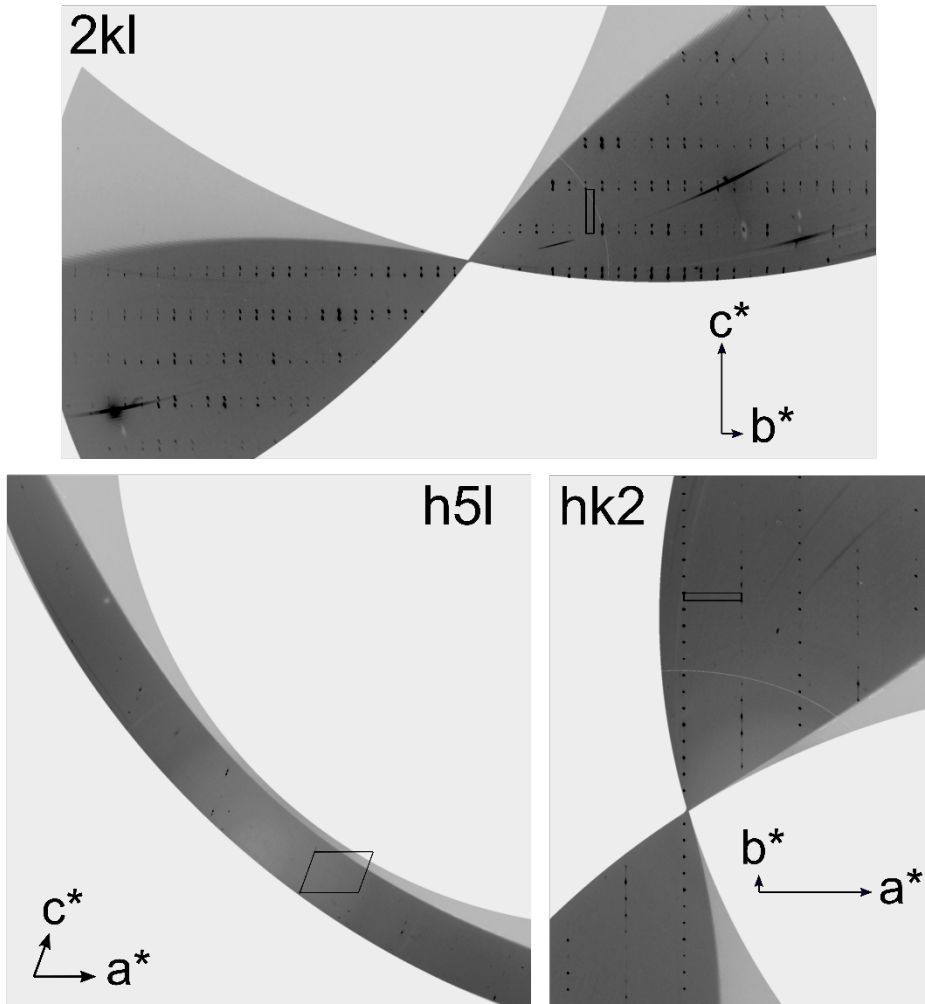
Reciprocal space reconstructions with the reciprocal unit cell indicated of  $\text{NaCl} \cdot 13\text{H}_2\text{O}$  at 1.5 GPa and 295 K, measured at P02.2 beamline at the DESY.

Fig. S4.



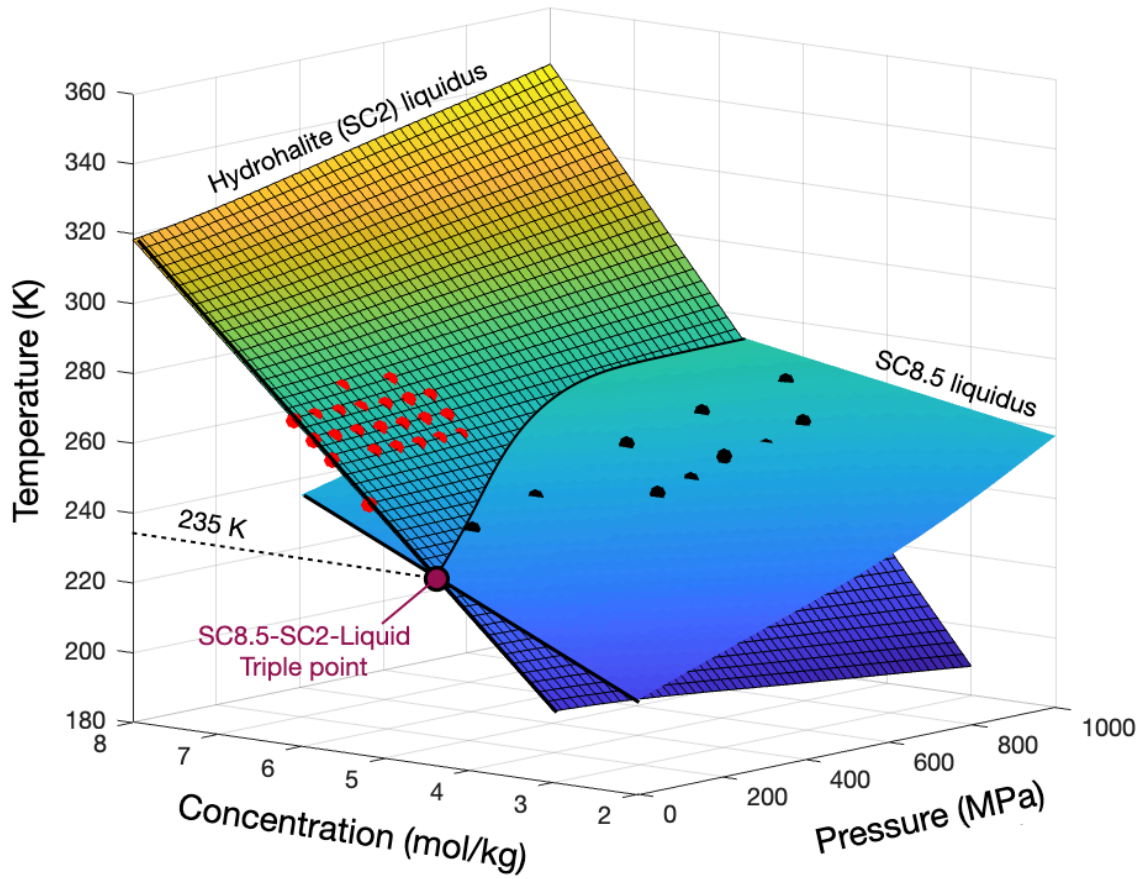
Crystal structure of sodium chloride decahydrate NaCl·13H<sub>2</sub>O (SC13). [Na(H<sub>2</sub>O)<sub>6</sub>]<sup>+</sup> units are represented by yellow colored octahedra; the spheres represent locations of Na<sup>+</sup> (yellow), Cl<sup>-</sup> (green) and, O (red), and solved hydrogen positions in pink. The dashed grey lines represent hydrogen bonding.

Fig. S5.



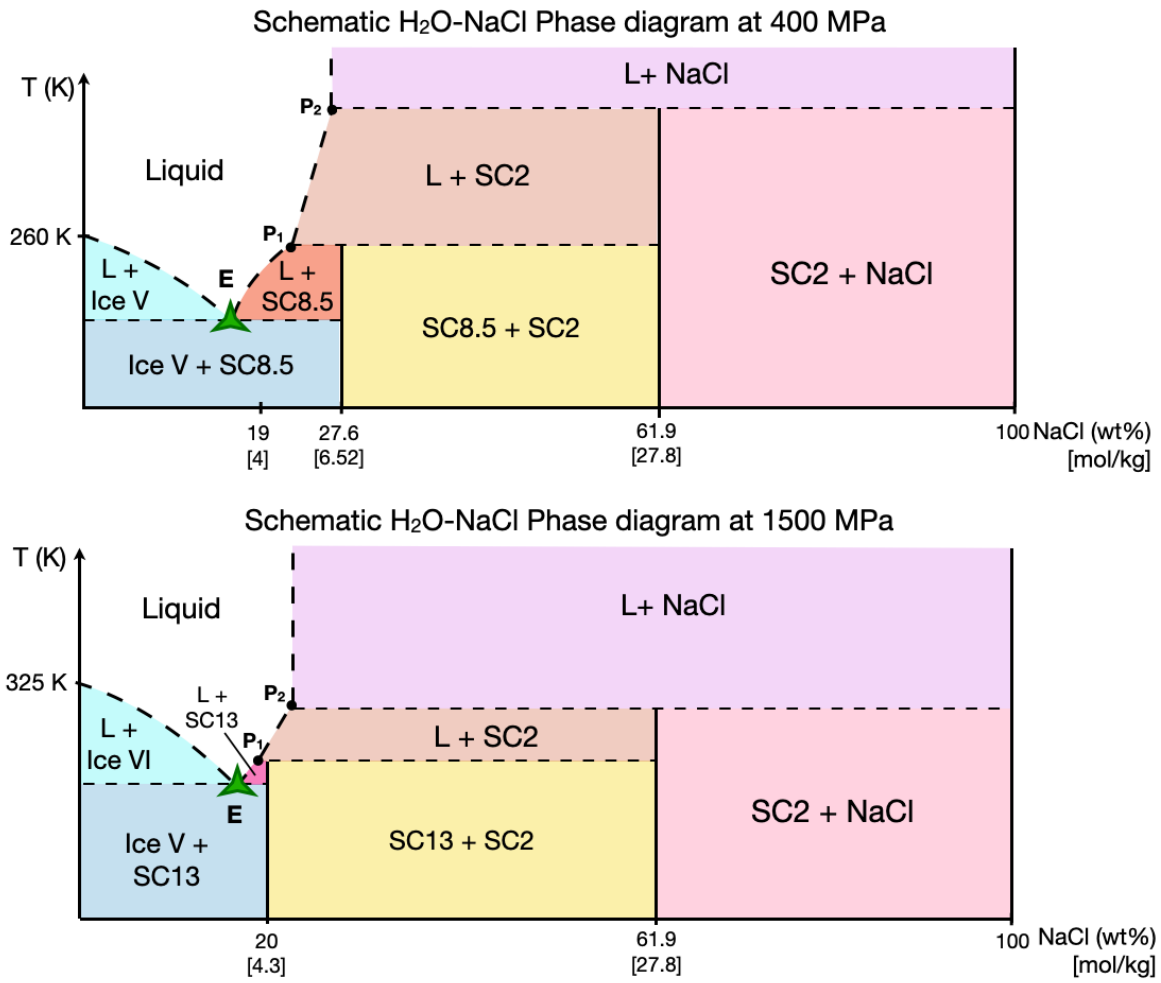
Reciprocal space reconstructions with the reciprocal unit cell indicated of the C2/c needle phase at 0.5 GPa and 238 K, measured at ID15B beamline at the ESRF. In the 2kl reconstruction, the presence of the second twin domain can be observed.

Fig.S6.



Liquidus surfaces of hydrohalite (SC2), and SC8.5 hydrates. The data from Sawamura et al., (2007) on SC2 are reported as red dots. The liquidus data from Valenti et al., (2012) at 5.7 mol/kg and the data from the present study at 4 mol/kg are shown as black dots. The SC8.5-SC2-liquid metastable triple point at 1 bar and 235K is indicated in purple.

Fig.S7.



Schematic phase diagrams of the H<sub>2</sub>O-NaCl at 400 MPa (top) and 1500 MPa (bottom). Dashed lines represent boundaries with currently unconstrained coordinates.

**Table S1.**

Experimental coordinates of identified phases. Liquidus measurements are indicated with an asterisk.

Experiment 1			Experiment 2			Experiment 3			Experiment 4		
P (MPa)	T(K)	Phase	P (MPa)	T(K)	Phase	P (MPa)	T(K)	Phase	P (MPa)	T(K)	Phase
500	238	C2/c Needles	280	220	SC8.5	360	240	SC8.5	420	238	C2/c Needles
450	243	SC8.5	290	225	SC8.5	450	240	SC8.5	380	240	SC8.5*
400	240	SC8.5	340	230	SC8.5	450	248	SC8.5*	310	230	SC8.5
			360	235	SC8.5	700	248	SC8.5	280	220	SC8.5
			390	240	SC8.5	800	260	SC8.5*	270	205	SC8.5
			470	245	SC8.5	1070	268	SC8.5+ice VI	230	190	SC8.5
			530	250	SC8.5*	1210	270	SC8.5+ice VI	230	170	SC8.5
			610	255	SC8.5*	1230	274	SC8.5+ice VI	150	150	SC8.5
			500	225	SC8.5	1230	275	SC2 + ice VI	100	150	SC8.5
			690	230	SC8.5	1580	290	SC13+ice VI	25	150	SC8.5
			660	235	SC8.5	1590	294	SC13+ice VI	23	183	SC8.5
			660	240	SC8.5	2150	299	SC13+ice VI	28	210	SC8.5
			660	245	SC8.5	2080	300	SC13+ice VI	19	240	SC2+ice Ih
			710	255	SC8.5*	2140	285	SC13+ice VI			
			1330	255	SC8.5	1690	300	SC13*			
			2150	245	SC8.5	1000	265	SC2+ice VI			
			1860	265	SC13+ice VI	1200	265	SC2+ice VI			
			1770	285	SC13+ice VI	1610	265	SC2+ice VI			
			1550	295	SC13*	2140	265	SC2+ice VI			
			1650	290	SC13	2300	265	ice VII + NaCl			
			1500	280	SC13+ice VI						
			1670	270	SC13+ice VI						
			1860	300	SC13+ice VI						
			1970	305	SC13+ice VI						

**Table S2.**

Crystallographic data and refinement parameters for the NaCl hydrates discovered at low-temperature–high-pressure conditions

Crystal data	2NaCl·17H <sub>2</sub> O SC8.5	NaCl·13H <sub>2</sub> O SC13
Pressure, MPa	450	1500
Temperature, K	243	295
Space group	<i>C2/c</i>	<i>I2/m</i>
<i>a</i> , Å	15.0132(4)	10.9150(8)
<i>b</i> , Å	6.08030(10)	11.8900(10)
<i>c</i> , Å	21.9946(18)	11.2752(5)
$\beta$ , °	103.086(5)	118.307(7)
Volume, Å <sup>3</sup>	1955.63(18)	1288.30(17)
Wavelength	0.41112	0.2897
Max. $\theta$ °	16.573	17.591
Index ranges	-20 < <i>h</i> < 20 -8 < <i>k</i> < 8 -17 < <i>l</i> < 19	-16 < <i>h</i> < 13 -14 < <i>k</i> < 16 -22 < <i>l</i> < 23
No. meas. refl.	1803	2606
No. uniq. refl.	1024	1512
No. obs. refl ( $I > 2\sigma(I)$ )	911	1362
No. parameters	109	96
$R_{\text{int}}$	0.0373	0.0314
$R_1$ , all data	0.0598	0.0517
$R_1$ , $I > 2\sigma(I)$	0.0562	0.0546
w $R_2$ , all data	0.1772	0.1439
w $R_2$ , $I > 2\sigma(I)$	0.1670	0.1382
GooF	1.081	1.146
$\Delta\rho_{\text{max}}/\Delta\rho_{\text{min}}$ (e.Å <sup>-3</sup> )	0.34/-0.29	0.368/-0.3

**Table S3.**

Refined hydrogen bonds for the crystal structure of  $2\text{NaCl}\cdot 17\text{H}_2\text{O}$  at 0.45 GPa and 243 K.

	D-H	H...A	D...A	<(DHA)
O1-H1A...O	0.846(10)	1.955(11)	2.800(3)	179(6)
O2-H2A...O9	0.853(10)	1.992(15)	2.819(3)	163(4)
O5-H5A...Cl	0.846(10)	2.39(2)	3.179(3)	156(5)
O6-H6A...O7	0.847(10)	2.02(1)	2.856(3)	169(4)

**Table S4.**Refined hydrogen bonds for the crystal structure of NaCl·13H<sub>2</sub>O at 1.5 GPa and 295 K.

	D-H	H...A	D...A	<(DHA)
O2-H2A...O7	0.840(10)	1.960(11)	2.7877(17)	168(2)
O3-H3B...O8	0.856(10)	2.072(11)	2.9096(18)	166(3)
O6-H6A...Cl	0.869(10)	2.33(2)	3.1235(11)	152(3)
O7-H7B...O1	0.854(9)	2.15(2)	2.8429(15)	138(2)
O7-H7A...Cl	0.852(9)	2.449(16)	3.1725(10)	143(2)
O8-H8...O1	0.854(10)	2.36(5)	2.822(2)	114(4)

**Dataset S1 (separate file).** The Crystallographic Information Files (CIFs) of Disodium chloride decahydrate,  $2\text{NaCl}\cdot 17\text{H}_2\text{O}$ , (SC8.5) and sodium chloride decahydrate,  $\text{NaCl}\cdot 13\text{H}_2\text{O}$  (SC13) are attached separately to this manuscript. They are also available on the Inorganic Crystal Structure Database (ICSD) under deposition numbers CSD 2203504-2203505

### SI References

1. G. M. Sheldrick, Crystal structure refinement with SHELXL. *Acta Crystallogr. Sect. C Struct. Chem.* **71**, 3–8 (2015).
2. C. B. Hübschle, G. M. Sheldrick, B. Dittrich, ShelXle: a Qt graphical user interface for SHELXL. *J. Appl. Crystallogr.* **44**, 1281–1284 (2011).
3. P. Valenti, R. J. Bodnar, C. Schmidt, Experimental determination of  $\text{H}_2\text{O}$ – $\text{NaCl}$  liquid to 25mass%  $\text{NaCl}$  and 1.4GPa: Application to the Jovian satellite Europa. *Geochim. Cosmochim. Acta* **92**, 117–128 (2012).
4. S. Sawamura, N. Egoshi, Y. Setoguchi, H. Matsuo, Solubility of sodium chloride in water under high pressure. *Fluid Phase Equilibria* **254**, 158–162 (2007).
5. J. M. Brown, Local basis function representations of thermodynamic surfaces: Water at high pressure and temperature as an example. *Fluid Phase Equilibria* **463**, 18–31 (2018).
6. L. Adams, Equilibrium in binary systems under pressure. I. An experimental and thermodynamic investigation of the system,  $\text{NaCl}$ – $\text{H}_2\text{O}$ , at  $25^\circ$ . *J. Am. Chem. Soc.* **53**, 3769–3813 (1931).